Genomics 115 (2023) 110664

Contents lists available at ScienceDirect

Genomics

journal homepage: www.elsevier.com/locate/ygeno

Transcriptome profiling revealed that key rumen epithelium functions change in relation to short-chain fatty acids and rumen epithelium-attached microbiota during the weaning transition

Koki Nishihara [a,1], Jolet van Niekerk [b,1], David Innes [a], Zhixiong He [c,d], Angela Cánovas [e], Le Luo Guan [b], Michael Steele [a,*]

[a] Department of Animal Biosciences, Animal Science and Nutrition, University of Guelph, Guelph, ON N1G 1Y2, Canada
[b] Department of Agricultural, Food and Nutritional Science, University of Alberta, Edmonton, AB T6G 2P5, Canada
[c] CAS Key Laboratory for Agro-Ecological Processes in Subtropical Region, National Engineering Laboratory for Pollution Control and Waste Utilization in Livestock and Poultry Production, South-Central Experimental Station of Animal Nutrition and Feed Science in Ministry of Agriculture, Hunan Provincial Engineering Research Center for Healthy Livestock and Poultry Production, Institute of Subtropical Agriculture, The Chinese Academy of Sciences, Changsha 410125, China
[d] University of Chinese Academy of Sciences, Beijing 100049, China
[e] Centre for Genetic Improvement of Livestock, Department of Animal Biosciences, University of Guelph, Guelph, ON N1G 2W1, Canada

ARTICLE INFO

Keywords:
Rumen biopsy
Weaning transition
Short-chain fatty acids
Rumen transcriptome
Rumen epithelium-attached microbes

ABSTRACT

This study aims to characterize the functional changes of the rumen epithelium associated with ruminal short-chain fatty acid (SCFA) concentration and epithelium-attached microbes during the weaning transition in dairy calves. Ruminal SCFA concentrations were determined, and transcriptome and microbiota profiling in biopsied rumen papillae were obtained from Holstein calves before and after weaning using RNA- and amplicon sequencing. Metabolic pathway analysis showed that pathways related to SCFA metabolism and cell apoptosis were up- and down-regulated postweaning, respectively. Functional analysis showed that genes related to SCFA absorption, metabolism, and protective roles against oxidative stress were positively correlated with ruminal SCFA concentrations. The relative abundance of epithelium-attached *Rikenellaceae* RC9 gut group and *Campylobacter* was positively correlated with genes involved in SCFA absorption and metabolism, suggesting that these microbes can cooperatively affect host functions. Future research should examine the contribution of attenuated apoptosis on rumen epithelial functional shifts during the weaning transition.

1. Introduction

Cattle are ruminants distinct from monogastric animals due to their forestomaches (rumen, reticulum, and omasum). In the neonatal and preweaning phases, the small intestine plays a major role in nutrient absorption [1], similar to monogastric animals. During the weaning transition, the rumen becomes the major site of digestion and absorption [2]: symbiotic microbes in the rumen produce short-chain fatty acids (SCFA: acetate, propionate, and butyrate) by solid feed fermentation [3], and the rumen epithelium absorbs SCFA and metabolizes a proportion. SCFA absorbed from the rumen epithelium satisfies 80% of the ruminants' energy requirements [4]. Papillae development is promoted by SCFA [5,6], and this development could increase surface area for efficient SCFA absorption [1]. Therefore, functional development of the rumen during the weaning transition could directly affect feed intake and calf growth [7].

Undeveloped rumen papillae in preweaning could cause SCFA accumulation in the rumen with lower pH [8,9], which may result in lower organic matter fermentation [10] and compromised rumen health [11]. Therefore, rumen epithelium molecular pathways may respond to ruminal SCFA during the weaning transition. Although rumen molecular changes during the weaning transition have been studied [7,12,13], these studies only compared functional changes between different ages/diets and did not directly evaluate how epithelium functions respond to ruminal SCFA. In addition, these studies used samples collected from different animals. Thus, how the same individual's rumen epithelium responds to ruminal SCFA during the weaning transition remains unclear.

* Corresponding author at: Department of Animal Biosciences, University of Guelph, Guelph, ON N1G 2W1, Canada.
E-mail address: masteele@uoguelph.ca (M. Steele).
[1] K. Nishihara and J.K. van Niekerk contributed equally to this work.

https://doi.org/10.1016/j.ygeno.2023.110664
Received 18 January 2023; Received in revised form 12 May 2023; Accepted 31 May 2023
Available online 5 June 2023

Rumen microbiota could also affect calf growth because the composition of microbiota alters SCFA production [14,15]. However, these studies were based on digesta-associated microbiota, and some digesta-associated microbiota were different at sampling time points [16]. Epithelium-attached microbiota are distinct from digesta-associated microbiota [17,18] and may represent the relationship between ruminal microbiota and host function (i.e. SCFA absorption and metabolism) because they are directly attached to the epithelium. Epithelium-attached microbiota also have positive effects on host health and productive performance [19–21], and they may positively affect the host's rumen function during the weaning transition. Furthermore, rumen epithelium-attached bacteria postweaning are more diverse than during preweaning [22], and some bacteria may be associated with higher ruminal SCFA concentration and greater papillae surface area postweaning [22–24]. However, host-epithelial attached microbial interactions at the molecular level remain unclear.

We previously reported on calf traits (ruminal SCFA concentration, papillae histology, and calf starter intake (CSI)), rumen epithelium-attached microbiota, and their correlation obtained from the same individuals during the weaning transition [9,22]. Rumen epithelium transcriptomic analysis with these calf traits and epithelium-attached microbiomes could fill in the above knowledge gaps regarding the weaning transition. The objective of this study is to characterize the functional changes of the rumen epithelium transcriptome associated with ruminal SCFA concentration and the epithelium-attached microbes during the weaning transition. To achieve our purpose, differentially expressed (DE) genes analysis and weighted correlation network analysis (WGCNA) [25] – an approach that can find highly correlated genes clusters (modules) and related gene modules to the sample traits – were performed on the samples obtained from our previous studies [9,22] during the weaning transition. We hypothesized that candidate functional genes involved in SCFA absorption and metabolism respond to higher ruminal SCFA concentrations, and epithelium-attached bacteria and these genes cooperatively affect rumen function.

2. Materials and methods

2.1. Animals and housing

Animals, housing, and feeding were described in a previous study [9]. In brief, six Holstein bull calves were cared for and handled in accordance with the Canadian Council on Animal Care [26] regulations and all experimental procedures were reviewed and approved by the institutional Animal Care and Use Committee (University of Alberta, AB; AUP00002010). Briefly, calves were individually housed in a barn with pens (3.05 × 3.66 m) with rubber mats (2.42 × 2.42 m) and wood shavings. Calves were fed 3 L of milk replacer (MR; 150 g/L, 26% crude protein (CP), 20% fat, 38% lactose as fed; Grober Nutrition, Cambridge, Ontario) solution twice daily for the first week of life. Thereafter, MR solution was fed at 15% of body weight (BW; adjusted every 7 days based on new BW) per day in 2 equal volumes. During week 6, calves received 50% of the previous week's MR allocation and were fully weaned at the end of week 6. Calves had ad libitum access to texturized calf starter (CS; 23.4% CP, 32.9% starch; Trouw Nutrition Canada Inc., Strathmore, AB, Canada), straw (4.1% CP, 1.7% starch, 75.7% neutral detergent fiber; Skyline Harvest, Blumenort MB, Canada, 1-in. chop length) and water from week 2. Individual intakes of MR, CS, straw and water were recorded daily and described in a previous study [9].

2.2. Sample collection

Ruminal SCFA concentrations, papillae histology, and CSI used in further WGCNA were obtained from Table 2, 3, and Fig. 1 of our previous study [9]. Ruminal tissue biopsies were collected 3 h after the morning feeding at the end of week 5 (W5), 7 (W7), and 12 (W12), as described by van Niekerk et al. [27]. Briefly, calves were not sedated, but were restrained in a calf chute during sampling. An Allis clamp (15 cm, Jorvet, Loveland, CO) was used to retrieve the dorsal coronary pillar through the cannula opening for ruminal tissue sampling. This exposed the caudodorsal blind sac for sampling, which was done using surgical scissors. To ensure that whole papillae were obtained, the cut was made below the base of the papillae. After the samples were obtained, the tissue was washed with sterile phosphate-buffered saline (pH 7.4). For histological analysis, two ruminal tissue samples at each time point were submerged in 10% formalin solution and stored at room temperature. An additional four ruminal tissue samples were placed in RNA stabilization fluid (RNALater, ThermoFisher Scientific, Burlington, ON, Canada) for further analysis, and the samples were stored at room temperature for 24 h and then frozen at −20 °C. The ruminal tissue samples in formalin solution were used to measure rumen papillae surface area, length, and width, and rumen papillae surface area, length, and width were analyzed as described previously [9]. The papillae length was measured from the tip to the base, and its width was measured at the halfway of each papilla. The 2-sided papillae surface area was determined by tracing the papillae from base to base and then multiplying it by 2. Ruminal fluid was sampled through the cannula using a plastic tube and a syringe 3 h after the morning feeding at the end of W5, W7, and W12. Ruminal contents were filtered through 4 layers of cheesecloth, and 5 mL of ruminal fluid was frozen and stored at −20 °C for SCFA analysis. The concentrations of acetate, propionate, and butyrate were measured, and the concentration of ruminal total SCFA and the proportion of each SCFA were calculated and analyzed by van Niekerk et al. [9]. Ruminal SCFA concentrations, papillae histology, and CSI at W5, W7, and W12 of each calf were used for further WGCNA.

2.3. RNA extraction, library construction, and RNA-sequencing of rumen epithelium

A RNeasy mini kit (QIAGEN Inc., Germantown, MD, USA) was used to isolate total RNA from each biopsy sample (average total RNA concentration was 15,526 ± 6511 ng/sample), as per the manufacturer's instructions. RNA quality was evaluated using the RNA integrity number value and quantified by an ND-1000 Nanodrop Spectrometer (Thermo Scientific, Pittsburgh, PA) [28]. The RNA integrity number values were 8.9 ± 0.13 in all samples [27], indicating good RNA quality [28]. Library Construction was performed using the TruSeq RNA Library Prep Kit v2 sample preparation kit (Illumina, San Diego, CA) [29]. Adapters were ligated to the ends of double-stranded cDNA and PCR amplified to create libraries. Thereafter, cDNA libraries were pooled and then sequenced at Génome Québec Innovation Centre (Montréal, Quebec, Canada) using the Illumina HiSeq 4000 system (Illumina) which generated paired end-reads of 2 × 100 bp.

2.4. mRNA mapping, normalization, principal component analysis, and gene names annotation

Quality control analysis was performed using FastQC (v0.11.4) [30]. Fastq-mcf set at quality score ≥ 20, and length ≥ 75 were used to trim and filter adapters and low-quality bases from the obtained sequences [31]. Then, the clean sequencing reads were aligned to the bovine reference genome (UMD 3.1; Ensembl v.83.31) and assembled [32] using software packages TopHat2 (v2.0.9) [33] and Bowtie2 (v2.3.3.1) [34]. The BAM files generated by TopHat2 were then converted into SAM files using Samtools (v1.1) [35]. Thereafter the number of mapped reads per gene in the SAM file was quantified using HTSeq-count (v0.6.1) [36]. All sequences passed the quality control analysis including GC content, ambiguous base content, Phred score, base coverage, nucleotide contributions, and over-represented sequence parameters [37]. The mapped reads were normalized using counts per million (CPM), which are as follows: (number of reads mapped to a gene in a sample) ÷ (total number of reads mapped to all annotated genes in a sample) × 10^6. Genes were considered expressed when CPM > 1 and in

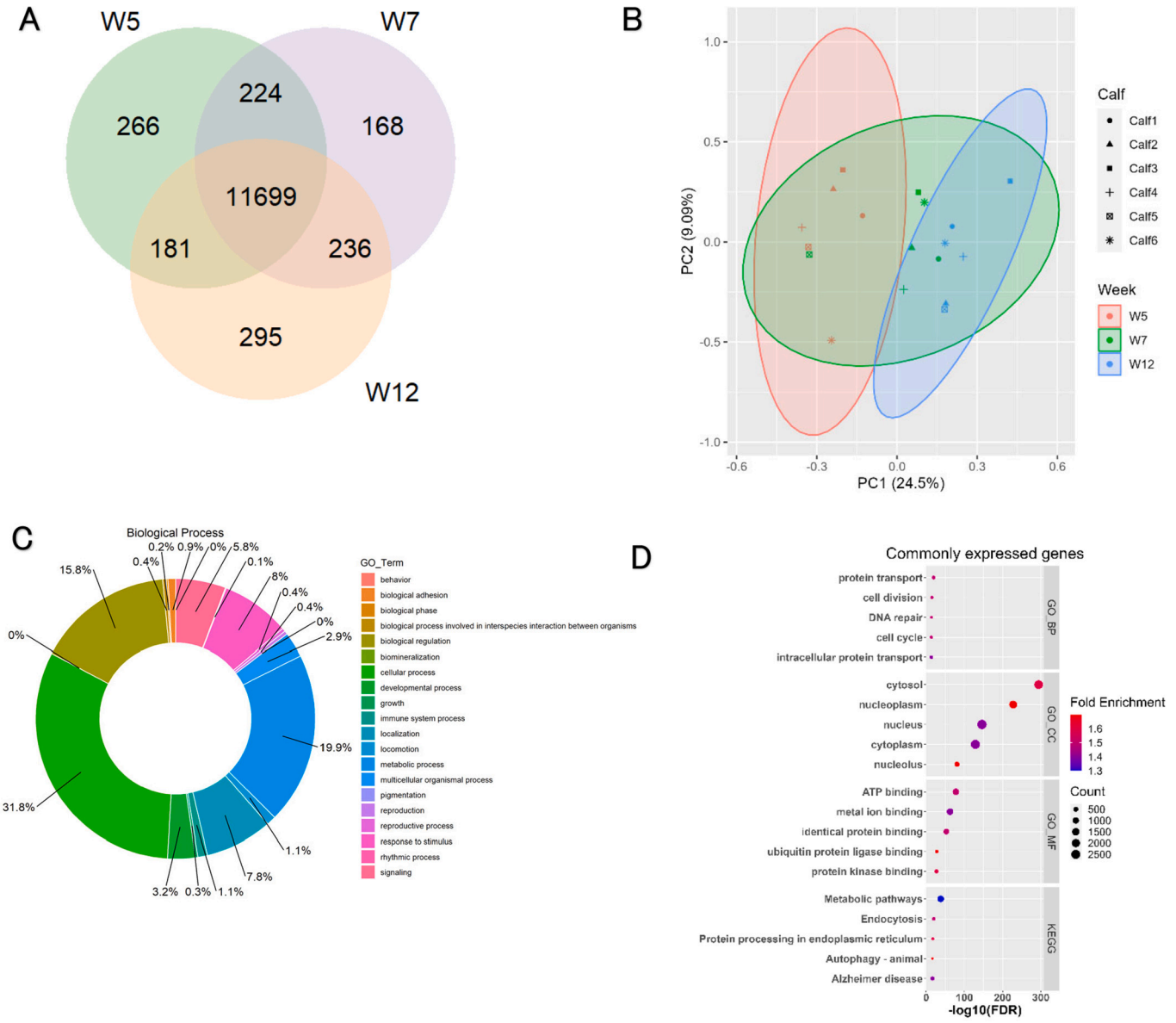

Fig. 1. Overview of epithelial transcriptome. (A) Venn diagram of the rumen epithelial expressed genes among W5, W7, and W12. (B) PCA plot of the rumen epithelial transcriptomes in each calf. Frames of each age were generated by setting frame.type as norm in ggfortify library's autoplot function. (C) Biological processes of commonly expressed genes among W5, W7, and W12 as identified by PANTHER. (D) Top 5 biological processes, cellular components, molecular function, and pathways of commonly expressed genes among W5, W7, and W12 as identified by DAVID.

at least four animals in at least one age group. The principal component analysis (PCA) was performed to see the general discrimination of expressed genes using ggfortify (v0.4.14) package in the R software (v4.1.3). Associated gene name annotation was performed using biomaRt [38] (v2.50.3) package in R software.

2.5. Differential expression analysis and WGCNA

Bioconductor edgeR (v3.36.0) package in R software was used to identify DE genes based on the pairwise comparison (W5 vs. W7, W7 vs. W12, and W5 vs. W12) [39]. Genes with $|\log_2$ fold change (logFC)$| > 1.3$ and adjusted *p*-values (false discovery rate (FDR) using the Benjamini and Hochberg (BH) method) < 0.05 were considered DE genes and selected for further functional analysis. To examine the relationship between expressed genes and phenotypic measures (concentration of ruminal total SCFA, acetate, propionate, and butyrate, rumen papillae surface area, length, and width) at W5, W7, and W12, the WGCNA package (v1.71) [39,40] in R software was used to identify the co-expressed genes correlated with the traits. Genes considered expressed were normalized by Log2 transformed (Log2(CPM + 1)) and inputted to WGCNA [40,41]. Sample clustering based on expressed genes showed no outliers in 18 samples (Fig. S1A), therefore no samples were removed in WGCNA. When RsquaredCut was set at 0.85 and networkType was assigned as singed using pickSoftThreshold function, the minimum power value was 16 (Fig. S1B). The power value was set to 16 because connectivity distribution was decrescent and the network was considered following the scale-free topology criterion (Fig. S1C–E). The co-expressed genes were grouped into modules (distinguished by different colour names) using the automatic one-step function, blockwiseModules with the following parameters: networkType = signed and minModuleSize = 60. The other parameters in pickSoftThreshold and blockwiseModules functions were followed by default. The modules were then used to identify module–trait relationships (calculated by Pearson correlation) with concentration of ruminal total SCFA, acetate,

propionate, butyrate, and rumen papillae surface area, length, width and CSI obtained from a previous study [41]. The gene modules with $p < 0.05$ and $|r| \geq 0.6$ were considered significantly and strongly correlated to a trait.

2.6. Functional analysis

The functions of genes commonly expressed among W5, W7, and W12 and uniquely expressed genes in each time-point were analyzed using the Protein Annotation Through Evolutionary Relationship (PANTHER) [42] gene tool. Metabolic pathway analysis of significant DE genes was performed using Ingenuity Pathway Analysis (IPA; QIAGEN Redwood City, www.qiagen.com/ingenuity). Ingenuity canonical pathways significantly enriched ($p < 0.05$, and |z-score| > 2) were sorted by p-value in ascending order, and the top 5 were considered up- and down-regulated pathways. Database for Annotation, Visualization, and Integrated Discovery (DAVID) (v2022q3) [43] was used for commonly expressed genes among W5, W7, and W12, uniquely expressed genes in each time-point, and the top WGCNA gene modules, which positively and negatively correlated with calf traits. The GO terms associated with the 3 main GO categories (biological processes, molecular function, and cellular component) were analyzed [44,45] and Kyoto Encyclopedia of Genes and Genomes (KEGG) pathways (FDR < 0.05 and fold enrichment >1) were sorted by FDR in ascending order, and the top 5 were considered as significantly enriched [46].

2.7. Correlation analysis between epithelium-attached bacteria and host transcriptome

The abundance of rumen epithelium-attached bacteria in genera level were obtained from 4 calves in each time-point, as described in a previous study [22]. Genera with relative abundance $\geq$0.1% in $\geq$2 animals in at least one group were used for Spearman's rank correlation analysis. Genes included in the gene modules which were positively and negatively correlated with ruminal SCFA concentration and in DE genes were also used for correlation analysis. Correlation was calculated using Hmisc (v4.7.1) and visualized using pheatmap (v1.0.12) packages in R software [47,48]. Raw p-values were adjusted using the BH method. Only correlations with $|r| \geq 0.6$ and FDR < 0.05 were considered as strongly and statistically significant.

3. Results

3.1. Overview of calf rumen transcriptome during weaning

A total of 13,069 genes were expressed (CPM > 1 and in >4 out of 6 animals per age group) in the rumen tissue of calves (Fig. 1A and Table S2). The number of expressed genes in W5, W7, and W12 were 12,370, 12,327, and 12,411, respectively. The number of commonly expressed genes among each age was 11,699, and the number of uniquely expressed genes was 266, 168, and 295 in W5, W7, and W12, respectively (Tables S3-S6). The PCA plot (Fig. 1B) showed that W5 and W12 clustered differently, but the cluster of W7 overlapped with that of W5 and W12. The annotation of commonly expressed and uniquely expressed genes using PANTHER (Fig. 1C) showed that the top biological processes in commonly expressed genes were "cellular process," "metabolic process," and "biological regulation," which included 31.8, 19.9, and 15.8%, respectively. The top biological processes in W5, W7, and W12 uniquely expressed genes were also "cellular process", "metabolic process", and "biological regulation" (Fig. S2). Annotation using DAVID showed that "Metabolic pathway" was a significantly enriched pathway (FDR < 0.05) in commonly expressed genes (Fig. 1D). Only "calcium ion binding" was significantly enriched (FDR < 0.05 and Fold enrichment $= 3$) in molecular function GO category of W12 uniquely expressed genes. No GO terms and metabolic pathways were annotated in W5 and W7 uniquely expressed genes.

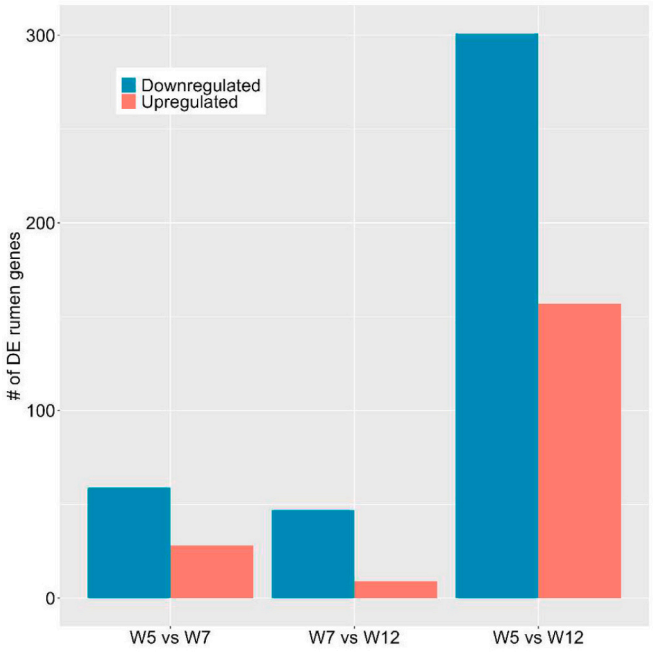

Fig. 2. The number of up-regulated (red) and down-regulated (blue) DE genes in W5 vs W7, W7 vs W12, and W5 vs W12. (For interpretation of the references to colour in this figure legend, the reader is referred to the web version of this article.)

Table 1
Top 5 metabolic pathways significantly enriched using IPA ($p < 0.05$, and |z-score| > 2).

Ingenuity canonical pathways	-log(p-value)	z-score	Molecules
W5 vs W12			
LXR/RXR Activation	4.93	2.53	*ABCG1,C3,CCL2,IL36A, IL36B,IL36G,IL36RN,LBP, RBP4,S100A8*
Adrenomedullin signaling pathway	2.62	−2.33	*C3,GNA15,IL36A,IL36B, IL36G,IL36RN,KCNN4,NPR2, PIK3C2G*
IL-6 Signaling	2.60	−2.45	*A2M,IL36A,IL36B,IL36G, IL36RN,LBP,PIK3C2G*
Toll-like Receptor Signaling	2.27	−2.00	*IL36A,IL36B,IL36G,IL36RN, LBP*
p38 MAPK Signaling	2.11	−2.45	*IL36A,IL36B,IL36G,IL36RN, PLA2G4D,PLA2G4F*
W5 vs W7			
SPINK1 Pancreatic Cancer Pathway	7.52	2.45	*CPM,KLK10,KLK12,KLK13, KLK14,KLK9*
Intrinsic Prothrombin Activation Pathway	6.73	−2.24	*KLK10,KLK12,KLK13,KLK14, KLK9*
MSP-RON Signaling In Macrophages Pathway	4.48	−2.24	*KLK10,KLK12,KLK13,KLK14, KLK9*
MSP-RON Signaling In Cancer Cells Pathway	4.14	−2.24	*KLK10,KLK12,KLK13,KLK14, KLK9*

3.2. DE genes and functional analysis among ages

There were 87, 56, and 457 DE genes between W5 vs W7, W7 vs W12, and W5 vs W12, respectively (Fig. 2 and Tables S7-S9). Among them, 28 were up-regulated and 59 were down-regulated in W7 compared to W5, 9 were up-regulated and 47 were down-regulated in W12 compared to W7, and 157 were up-regulated and 300 were down-regulated in W12 compared to W5. Functional analysis of DE genes using IPA showed the top significantly enriched metabolic pathways (Table 1). Among them, "LXR/RXR Activation", "Adrenomedullin

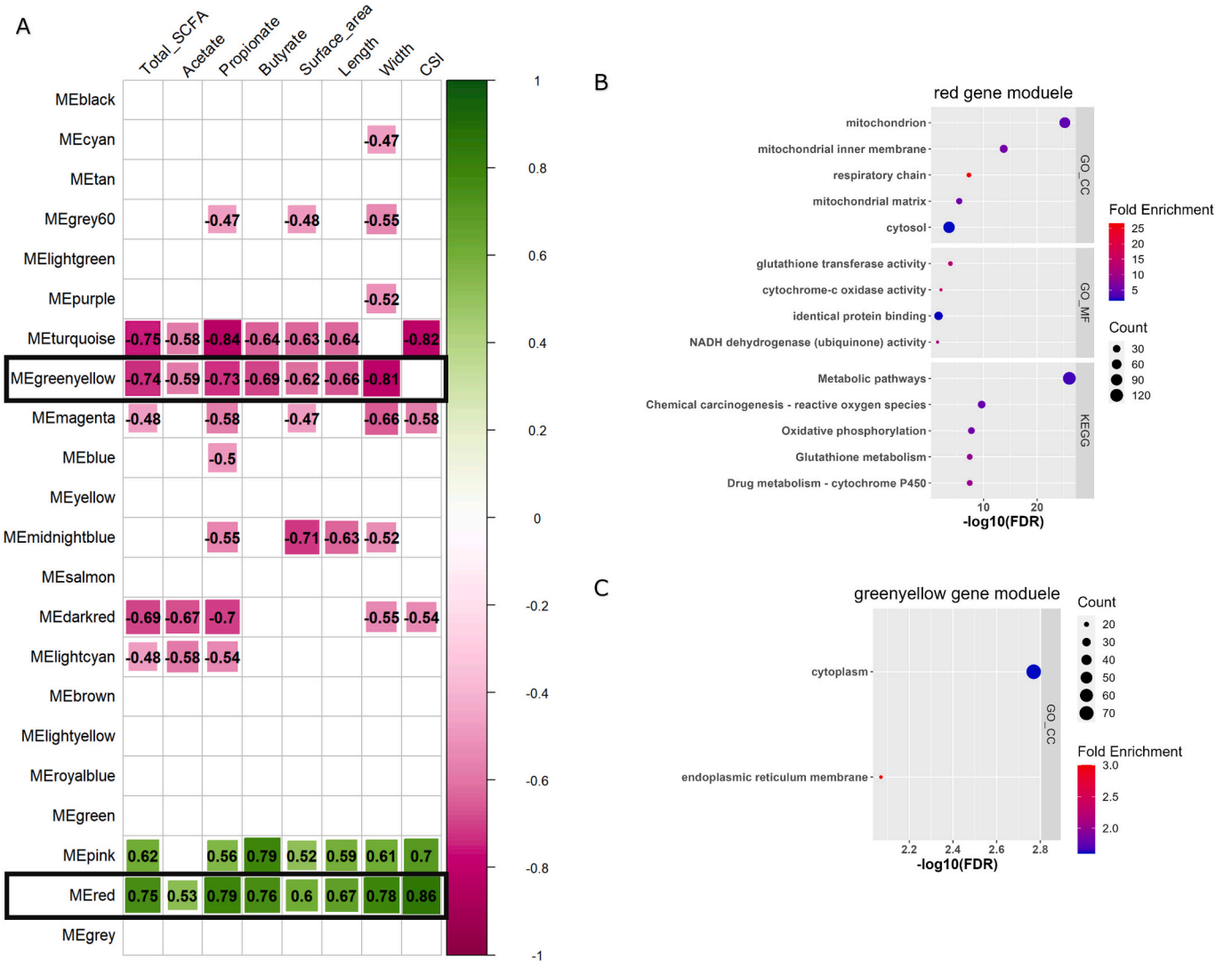

Fig. 3. Overview of WGCNA. (A) WGCNA identification of rumen epithelial gene modules correlated with the trait (concentration of ruminal total SCFA, acetate, propionate, and butyrate, rumen papillae surface area, length, width, and CSI). SCFA concentrations, papillae histology, and CSI were obtained from Table 2, 3, and Fig. 1 in our previous study [9]. Each module name is shown on the left, each trait is shown at the top, and the strength of the correlation is shown as a bar on the right in varying intensities of green (positive correlation, $r > 0$) or pink (negative correlation, $r < 0$). The correlation coefficients ($-1 < r < 1$) for each module and trait are shown in bold only when the p-value is <0.05. The gene modules (red and greenyellow, marked in black box) was significantly correlated with total SCFA, propionate, butyrate concentration, papillae surface area, length, and width. (B) Enriched cellular component, molecular function, and pathways in the red gene module as identified by DAVID. (C) Enriched cellular component in the greenyellow gene module as identified by DAVID. (For interpretation of the references to colour in this figure legend, the reader is referred to the web version of this article.)

signaling pathway", "IL-6 Signaling", "Toll-like Receptor Signaling", and "p38 MAPK Signaling" were the top 5 significant pathways in W5 vs W12. The "SPINK1 Pancreatic Cancer Pathway" was the top pathway in W5 vs W7. No pathways were found between W7 and W12.

3.3. Co-expression network analysis revealed relationships with rumen fermentation, rumen histology traits and calf starter intake at W5, W7, and W12

A total of 22 gene modules were identified using WGCNA (Fig. 3A and Tables S10–11). Gene modules (red and greenyellow), which mostly correlated to SCFA concentration and papillae histology, were selected for further functional analysis, correlation analysis and discussion. A gene module (red gene module, Table S12), including 498 co-expressed genes, was significantly and positively correlated with total SCFA, propionate, butyrate, rumen papillae surface area, length, width, and CSI ($p < 0.05$, and $r \geq 0.6$). A gene module (greenyellow gene module, Table S13), including 305 co-expressed genes, was significantly and negatively correlated with total SCFA, propionate, butyrate, rumen papillae surface area, length, and width ($p < 0.05$, and $r \leq -0.6$). DAVID annotation of these co-expressed genes showed the top significantly enriched (FDR < 0.05 and fold enrichment >1) cellular components, molecular functions, and pathways were "mitochondrion", "glutathione transferase activity", and "Metabolic pathways" in the red gene module, respectively (Fig. 3B), and "cytoplasm" was the top significantly enriched (FDR < 0.05 and fold enrichment >1) cellular component in the greenyellow gene module.

3.4. Functional candidate genes from epithelium-attached microbiota, gene module, and their correlations in rumen epithelium

Further analysis showed 103 and 12 DE genes were part of co-expressed genes in the red and the greenyellow gene modules, respectively (Tables S14–15). The genes in the red gene module and DE genes

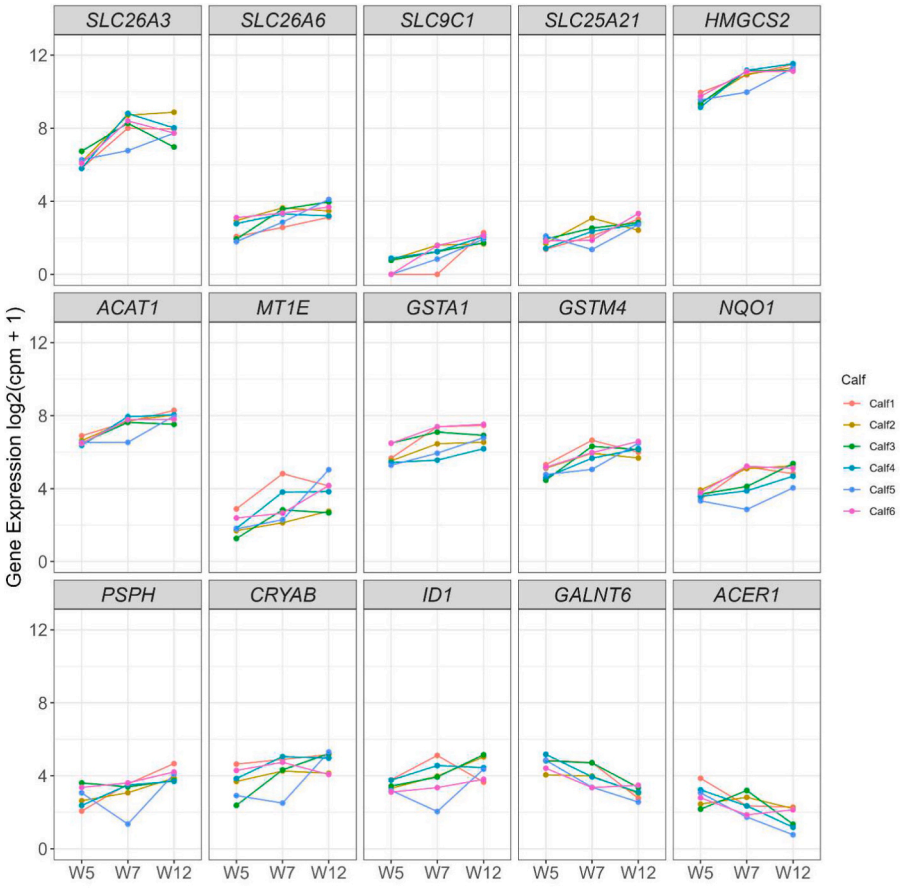

Fig. 4. Gene expression $\log_2(\text{CPM} + 1)$ of SCFA absorption (*SLC26A3*, *SLC26A6*, *SLC9C1*, and *SLC25A21*, included in the red gene module), metabolism (*HMGCS2*, and *ACAT1*, included in the red gene module), protective role against oxidative stress (*MT1E*, *GSTA1*, *GSTM4*, *NQO1*, *PSPH*, *CRYAB*, and *ID1*, included in the red gene module), and oxidative stress (*GALNT6* and *ACER1*, included in the greenyellow gene module) in DE genes. (For interpretation of the references to colour in this figure legend, the reader is referred to the web version of this article.)

Table 2
Significantly ($|r| > 0.6$, and FDR < 0.05) correlated bacteria with DE genes included in the red and greenyellow gene module.

Gene module	Gene	Bacteria	*r*	FDR
red	*CA12*	*Rikenellaceae* RC9 gut group	0.93	0.029
red	*SCGB1C1*	*Rikenellaceae* RC9 gut group	0.92	0.029
red	*ANAPC11*	*Rikenellaceae* RC9 gut group	0.92	0.030
red	*HMGCS2*	*Campylobacter*	0.62	0.031
red	*SLC30A10*	*Rikenellaceae* RC9 gut group	0.61	0.034
red	*CD3G*	*o_Betaproteobacteriales*	−0.74	0.006
red	*CLCN2*	*Bacteroides*	−0.65	0.022
greenyellow	*GPR82*	*Roseburia*	−0.86	0.024
greenyellow	*DMRT2*	*Pyramidobacter*	−0.63	0.028

included *solute carrier family 26 member 3* (*SLC26A3*), *solute carrier family 26 member 6* (*SLC26A6*), *solute carrier family 9 member C1* (*SLC9C1*), *solute carrier family 25 member 21* (*SLC25A21*), *3-hydroxy-3-methylglutaryl-CoA synthase 2* (*HMGCS2*), *acetyl-CoA acetyltransferase 1* (*ACAT1*) (related to SCFA absorption and metabolism), *metallothionein 1E* (*MT1E*), *glutathione S-transferase alpha 1* (*GSTA1*), *glutathione S-transferase mu 4* (*GSTM4*), *NAD(P)H quinone dehydrogenase 1* (*NQO1*), *phosphoserine phosphatase* (*PSPH*), *crystallin alpha B* (*CRYAB*), and *inhibitor of DNA binding 1* (*ID1*) (have protective roles against oxidative stress), and DE genes in the greenyellow module include *polypeptide N-acetylgalactosaminyltransferase 6 (GALNT6)* and *alkaline ceramidase 1 (ACER1)* (related to oxidative stress) (Fig. 4). The relative abundances of epithelium-attached microbiota in the rumen epithelium were obtained from our previous study [22]. The Spearman's rank correlations between DE genes included in gene modules (red and greenyellow) and epithelium-attached microbiota in rumen papillae are shown in Fig. S3 and Table 2. The relative abundance of *Rikenellaceae* RC9 gut group was significantly and positively correlated with *carbonic anhydrase 12* (*CA12*), *secretoglobin family 1C member 1* (*SCGB1C1*), *anaphase promoting complex subunit 11* (*ANAPC11*), and *solute carrier family 30 member 10* (*SLC30A10*) (FDR < 0.05, and $r \geq 0.6$) included in the red gene module. The relative abundance of *Campylobacter* was significantly and positively correlated with *HMGCS2* (included in the red gene module), and *o_Betaproteobacteriales*, *Bacteroides*, *Roseburia*, and *Pyramidobacter* were significantly and negatively correlated with *CD3 gamma subunit of T-cell receptor complex* (*CD3G*, included in the red gene module), *chloride voltage-gated channel 2* (*CLCN2*, included in the red gene module), *G protein-coupled receptor 82* (*GPR82*, included in the greenyellow gene module), and *doublesex and mab-3 related transcription factor 2* (*DMRT2*, included in the greenyellow gene module) (FDR < 0.05, and $r \leq -0.6$).

4. Discussion

The main energy source for ruminants is SCFA produced from microorganisms in the rumen [4]. The development of rumen papillae also is spurred by SCFA to improve SCFA absorption efficiency [45] and some of the absorbed SCFA are metabolized in the rumen epithelium [46]. The rumen papillae in the blind sac collected in this study are considered to be in contact with the SCFA because the calves in this study do not have a hay mat in the rumen as in adult cows, and the blind sac is submerged in the rumen fluid. In this study, we analyzed the samples collected at W5, W7 and W12, and the concentration of total SCFA was higher at W7 and W12 compared to W5 [9]. Therefore, the samples collected in this study represent the epithelium response to increment of ruminal SCFA concentration during the weaning transition. Our results provide new insights into the characterization of the rumen epithelium's

transcriptome and the functional response to SCFA and the host-epithelial attached microbial interactions during the weaning transition.

The rumen tissue experiences dramatic environmental changes, such as SCFA production by symbiotic microorganisms, during the weaning transition [47]. Therefore, GO terms and metabolic pathways related to SCFA absorption and metabolism were expected to be annotated after weaning. However, no GO terms or metabolic pathways related to SCFA absorption and metabolism were identified in uniquely expressed genes after weaning. In addition, there were no large differences in "metabolic process" percentage of uniquely expressed genes among ages. On the other hand, "Metabolic pathway" was significantly enriched in commonly expressed genes among different ages. The development of ketogenesis did occur in the absence of solid feed consumption [49]. Therefore, genes involved in ketogenesis may be expressed before W5. During the weaning transition, DE genes included in the gene modules (red and greenyellow) associated with ruminal SCFA concentration may play an important role in SCFA absorption and metabolism because ketogenesis capacity increased with age and SCFA concentration [49], and total SCFA concentrations were higher postweaning. Therefore, we discussed DE genes included in the gene modules (red and greenyellow) with the calf's traits as follows: CSI during the weaning transition increases the ruminal total SCFA concentration [48], and SCFA are absorbed by the rumen epithelium [50]; butyrate and some of the absorbed acetate are metabolized to acetoacetate or 3-hydroxybutyric acid in the rumen epithelium [51]. Therefore, we hypothesized that genes involved in SCFA absorption and metabolism respond to higher ruminal SCFA concentration.

Consistent with this hypothesis, we found that genes related to SCFA absorption (*SLC26A3*, *SLC9C1*, *SLC26A6*, and *SLC25A21*) and metabolism (*ACAT1* and *HMGCS2*) were included in DE genes and the red gene module, which positively correlated with SCFA concentration and CSI. *SLC26A3*, *SLC9C1*, *SLC26A6*, and *SLC25A21* act as exchanger of SCFA, bicarbonate, sodium, or proton [52–55]. In the rumen epithelium, *SLC26A3* was expressed higher when ruminants were fed high concentrate diets [56,57]. In beef cattle, *ACAT1* and *HMGCS2* catalyze the condensation of acetyl-CoA to generate hydroxymethylglutaryl-CoA [58]. Feed efficiency was associated with *ACAT1* expression in the rumen epithelium [59] and *HMGCS2* accelerates ketogenesis in the rumen epithelium [60]. The "LXR/RXR Activation" was the top activated pathway after weaning. Efflux of cholesterol is enhanced by LXR/RXR which act as a sensor of cholesterol [61,62], and LXR/RXR are controlled during high-grain feeding in nonlactating dairy cattle [63]. Acetyl-CoA synthesized from SCFA is a substrate of cholesterol synthesis and cholesterol accumulation could cause chronic stress and impaired cellular functions in lung cells [64]. These genes and metabolic pathways may be accelerated by higher SCFA concentration due to weaning and contribute to SCFA influx and efflux, acid neutralization, cholesterol homeostasis, and ketogenesis in the rumen epithelium during the weaning transition. However, rumen epithelial ketogenesis capacity was increased by both SCFA and aging in young ruminants [49]. To distinguish aging and SCFA effects, future studies need to analyze the effects of aging on these gene expressions. Also, genes localized in the mitochondria were abundant in the red gene module. Ketogenesis in the ruminal epithelium is performed exclusively in the mitochondria [65], and the cells of the strata basale and spinosum, which have a significant number of the mitochondria, contribute most to the ketogenesis properties of the tissue [66]. We previously reported that there is a positive week-related effect on the number of cells and thickness in the basale and spinosum layers [65–68]. In addition, we found that genes localized in the mitochondria were not abundant in the greenyellow gene module, which negatively correlated with SCFA concentration (Fig. 3C). Our findings suggested that the increment of the basale and spinosum layers during the weaning transition could contribute to higher SCFA metabolization efficiency. However, it is unclear whether the number of mitochondria in rumen papillae is higher during the weaning transition. Future studies are required to investigate the number of mitochondria and reveal the contribution of the mitochondria number to SCFA metabolism during the weaning transition.

It is important to note that we found genes that have protective roles against oxidative stress (*MT1E*, *GSTA1*, *GSTM4*, *NQO1*, *PSPH*, *CRYAB*, and *ID1*) which were included in DE genes and the red gene module. Among these genes, *MT1E*, *NQO1*, *PSPH*, and *ID1* are involved in protection against oxidative stress [67–70]. In several tissues and cell lines, *GSTA1* and *GSTM4*, a family of Glutathione S-transferase, play a crucial role in countering oxidative stress [71–73]. In addition, *CRYAB* can protect cardiomyocytes from oxidative stress-induced apoptosis [74]. We also found that *GALNT6* and *ACER1*, related to oxidative stress, were down-regulated postweaning and were included in the greenyellow gene module, which negatively correlated with ruminal SCFA concentration. In HT29 and LOVO cells, *GALNT6* was expressed lower by oxidative stress [75]. Deficiency of *alkaline ceramidase 3 (ACER3)*, one of the ACER family, attenuated apoptosis in nonalcoholic steatohepatitis liver by suppression of oxidative stress [76]. These results suggest that protective roles against oxidative stress could be accelerated in postweaning and in higher ruminal SCFA concentration. In addition, significant GO terms and metabolic pathways identified in the red gene module were related to adenosine triphosphate generation, reactive oxygen species (ROS) generation, and oxidative stress (Fig. 3B). It has been reported that butyrate uncoupled glycolytic input and allowed preferential fueling of oxidative phosphorylation in immune cells [77]. Oxidative phosphorylation is also a consequence of ROS generation, which contributes to both homeostatic signaling and oxidative stress [78], and excessive oxidative stress could induce cell apoptosis [79]. These data suggest that a higher butyrate concentration postweaning can accelerate oxidative phosphorylation in the rumen epithelium and can result in excessive oxidative stress, which induces cell apoptosis. To avoid apoptosis, genes involved in protective roles against oxidative stress (*MT1E*, *GSTA1*, *GSTM4*, *NQO1*, *PSPH*, *CRYAB*, and *ID1*) may respond to higher SCFA concentrations after weaning. This hypothesis is supported by the results of canonical pathway analysis: a pathway associated with apoptosis ("p38 MAPK Signaling") [80,81] was inactivated after weaning (Table 2). In addition, apoptosis was inhibited by butyric acid [82] and starter intake [83] and associated with rumen papillae length, and genes related to apoptosis were inhibited after weaning or solid diet fed calves in several studies [7,12,13]. Therefore, we propose that the inhibition of oxidative stress-induced apoptosis may contribute to papillae development resulting in effective SCFA absorption [80,81] during the weaning transition. Furthermore, these DE genes were included in the red gene module, which positively correlated with papillae surface area, length, and width. We also previously reported that papillae surface area, length, and width were 14.5, 4.6, and 3.3 times higher in W12 than those in W5 [81,82]. However, the number of apoptosis cells was not investigated in this research. It will be interesting to reveal the contribution of apoptosis inhibition to SCFA absorption during the weaning transition.

Some rumen attached bacteria were associated with higher ruminal SCFA concentration and greater papillae surface area postweaning [82,83]. We hypothesized that epithelium-attached bacteria and genes responding to higher ruminal SCFA concentration could cooperatively affect rumen function. As we hypothesized, the results suggested that some epithelium-attached bacteria may cooperatively affect rumen function with genes responding to SCFA during the weaning transition. We found that the abundance of *Rikenellaceae* RC9 gut group, thought to produce acetate as digestive-associated bacteria [84,85], was positively associated with *CA12*, included in a family of carbonic anhydrases which provide protons for Na^+/H^+ exchanger. The abundance of the hindgut mucosa-attached *Rikenellaceae* RC9 gut group was positively associated with acetate concentration in its digesta content [86]. High-grain feeding was also associated with the abundance of jejunal mucosa-attached *Rikenellaceae* RC9 gut group [87]. In the omasum, *CA12* is thought to contribute to acetate absorption [88]. Rumen epithelium-attached *Rikenellaceae* RC9 gut group may also produce acetate, and

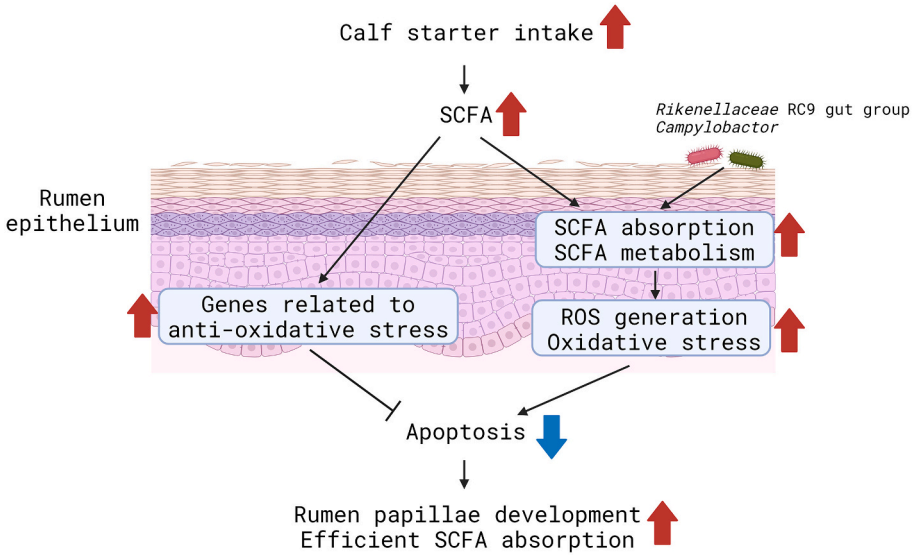

Fig. 5. Proposed rumen epithelium functional changes during weaning transition. The increment of ruminal SCFA concentration by calf starter intake could facilitate gene expressions related to SCFA absorption and metabolism. Some epithelium-attached bacteria may contribute to SCFA absorption and metabolism genes. Excessive SCFA metabolism could result in ROS generation and oxidative stress, which induce cell apoptosis. Genes related to anti-oxidative stress are simultaneously expressed higher after weaning and may suppress cell apoptosis induced by oxidative stress. This illustration was created using BioRender.com.

host transcriptome may respond to this to facilitate acetate absorption. However, *Rikenellaceae* RC9 gut group was not associated with ruminal acetate concentration in our previous study [87]. Epithelium-attached *Rikenellaceae* RC9 gut group abundance may not be associated with rumen fluid SCFA concentration. It will be important to determine whether epithelium-attached *Rikenellaceae* RC9 gut group produces acetate. We also found that the abundance of *Campylobacter* was also positively correlated with *HMGCS2*. To our knowledge, *Campylobacter* does not produce SCFA but is involved in oxygen scavenging [89]. The ruminal total SCFA were positively correlated with *Campylobacter* relative abundances in the rumen epithelium of goats [90]. Families of *Campylobacteraceae* bacteria were significantly more active in the epithelium of higher feed efficient cattle [21]. This suggests that *Campylobacter* may contribute to suitable ecological conditions for anaerobic communities, resulting in higher SCFA production, and potentially, host SCFA metabolism as a response. It will be interesting to reveal which epithelium-attached bacteria abundances are affected by *Campylobacter*. We also found that *Bacteroides*, o_*Betaproteobacteriales, Roseburia,* and *Pyramidobacter* were negatively associated with *CD3G* (included in red gene module), *CLCN2* (included in red gene module), *GPR82* (included in greenyellow gene module), and *DMRT2* (included in greenyellow gene module), respectively. The abundance of epithelium-attached *Bacrteroides* was negatively correlated with rumen epithelium thickness, and the abundances of *Roseburia* and *Pyramidobacter* were positively correlated with papillae surface area in our previous study [22]. However, we could not find the direct effect of these genes and bacteria on host function. Further studies are needed to reveal the contribution of these bacteria and genes to host function.

Our discussion assumes an influx of ruminal SCFA to the rumen epithelium. However, we did not evaluate the actual SCFA influx to the rumen epithelium and how its impact on rumen epithelium function. In addition, there is a possibility that the other factors triggered by ruminal SCFA accumulation or SCFA influx to the rumen epithelium could affect rumen epithelium function. Therefore, a future study using an in vitro model that controls SCFA influx is needed to evaluate the effect of SCFA influx on rumen epithelial function. Also, it should be noted that the number of animals used in this study ($n = 6$) was limited, and it will be important to perform WGCNA with larger numbers of animals in future studies.

5. Conclusion

Taken together, our data suggest that functions related to SCFA absorption, metabolism, and oxidative stress respond to higher ruminal SCFA concentrations during the weaning transition. Genes related to oxidative stress may play protective roles against oxidative stress-induced apoptosis due to higher SCFA concentration and may result in greater papillae histology, which contributes to higher SCFA absorption efficiency (Fig. 5). *Rikenellaceae* RC9 gut group and *Campylobacter* may cooperatively affect host SCFA absorption and metabolism with *CA12* and *HMGCS2* by producing acetate and creating a suitable environment for symbiotic anaerobic microbes. Further studies are needed to reveal the contribution of apoptosis inhibition in the rumen epithelium to SCFA absorption and to reveal the function of epithelium-attached bacteria and associated genes.

CRediT authorship contribution statement

Koki Nishihara: Conceptualization, Validation, Formal analysis, Methodology, Software, Visualization, Writing – original draft, Writing – review & editing. **Jolet van Niekerk:** Investigation, Validation, Data curation, Methodology, Writing – review & editing. **David Innes:** Writing – review & editing. **Zhixiong He:** Writing – review & editing. **Angela Cánovas:** Formal analysis, Methodology, Software, Writing – review & editing. **Le Luo Guan:** Conceptualization, Validation, Resources, Data curation, Formal analysis, Methodology, Funding acquisition, Writing – review & editing. **Michael Steele:** Conceptualization, Validation, Resources, Project administration, Supervision, Funding acquisition, Writing – review & editing.

Declaration of Competing Interest

None.

Data availability

All RNA-seq data were submitted to DDBJ, DRA database (BioProject Submission ID: PSUB019391, DRA accession: DRA015522, and BioProject ID: PRJDB15091).

Acknowledgements

The authors thank the Natural Sciences and Engineering Research Council of Canada (401436 to M. Steele, Ottawa, ON), Alberta Milk (Edmonton, AB, CA), Westgen (Abbotsford, BC, CA), BC Dairy Association (Burnaby, BC, CA), SaskMilk (Regina, SK, CA), Dairy Farmers of

Manitoba (Winnipeg, MB, CA), Trouw Nutrition (Guelph, ON, Canada), Lallemand Animal Nutrition (Montreal, QB, Canada) and Bayer Animal Health (Mississauga, ON, Canada), for the financial support provided for this study. The authors would also like to thank M. Middeldorp for assistance in calf management and care and sample collection and B. Tchir for assistance with calf management and care.

Appendix A. Supplementary data

Supplementary data to this article can be found online at https://doi.org/10.1016/j.ygeno.2023.110664.

References

[1] R.L. Baldwin, K.R. McLeod, J.L. Klotz, R.N. Heitmann, Rumen development, intestinal growth and hepatic metabolism in the pre- and postweaning ruminant, J. Dairy Sci. 87 (2004) E55–E65, https://doi.org/10.3168/jds.S0022-0302(04)70061-2.

[2] J. Dias, M.I. Marcondes, S. Motta de Souza, B. Cardoso da Mata e Silva, M. Fontes Noronha, R. Tassinari Resende, F.S. Machado, H. Cuquetto Mantovani, K. A. Dill-McFarland, G. Suen, Bacterial community dynamics across the gastrointestinal tracts of dairy calves during preweaning development, Appl. Environ. Microbiol. 84 (2018), https://doi.org/10.1128/aem.02675-17.

[3] J.B. Russell, J.L. Rychlik, Factors that alter rumen microbial ecology, Science 292 (2001) 1119–1122, https://doi.org/10.1126/science.1058830.

[4] E.N. Bergman, Energy contributions of volatile fatty acids from the gastrointestinal tract in various species, Physiol. Rev. 70 (1990) 567–590, https://doi.org/10.1152/physrev.1990.70.2.567.

[5] E.G. Sander, R.G. Warner, H.N. Harrison, J.K. Loosli, The stimulatory effect of sodium butyrate and sodium propionate on the development of rumen mucosa in the young calf, J. Dairy Sci. 42 (1959) 1600–1605, https://doi.org/10.3168/jds.S0022-0302(59)90772-6.

[6] H. Tamate, A.D. McGilliard, N.L. Jacobson, R. Getty, Effect of various dietaries on the anatomical development of the stomach in the calf, J. Dairy Sci. 45 (1962) 408–420. https://www.sciencedirect.com/science/article/pii/S0022030262894065.

[7] Y.-H. Kim, N. Toji, K. Kizaki, S. Kushibiki, T. Ichijo, S. Sato, Effects of dietary forage and calf starter on ruminal pH and transcriptomic adaptation of the rumen epithelium in Holstein calves during the weaning transition, Physiol. Genomics 48 (2016) 803–809, https://doi.org/10.1152/physiolgenomics.00086.2016.

[8] J.R. Aschenbach, G.B. Penner, F. Stumpff, G. Gäbel, Ruminant nutrition symposium: role of fermentation acid absorption in the regulation of ruminal pH, J. Anim. Sci. 89 (2011) 1092–1107, https://doi.org/10.2527/jas.2010-3301.

[9] J.K. van Niekerk, M. Middeldorp, L.L. Guan, M.A. Steele, Preweaning to postweaning rumen papillae structural growth, ruminal fermentation characteristics, and acute-phase proteins in calves, J. Dairy Sci. 104 (2021) 3632–3645, https://doi.org/10.3168/jds.2020-19003.

[10] M. Cerrato-Sánchez, S. Calsamiglia, A. Ferret, Effects of time at suboptimal pH on rumen fermentation in a dual-flow continuous culture system, J. Dairy Sci. 90 (2007) 1486–1492, https://doi.org/10.3168/jds.S0022-0302(07)71634-X.

[11] J.L. Kleen, G.A. Hooijer, J. Rehage, J.P.T.M. Noordhuizen, Rumenocentesis (rumen puncture): a viable instrument in herd health diagnosis, Dtsch. Tierarztl. Wochenschr. 111 (2004) 458–462. https://www.ncbi.nlm.nih.gov/pubmed/15648614.

[12] E.E. Connor, R.L. Baldwin 6th, C.-J. Li, R.W. Li, H. Chung, Gene expression in bovine rumen epithelium during weaning identifies molecular regulators of rumen development and growth, Funct. Integr. Genomics 13 (2013) 133–142, https://doi.org/10.1007/s10142-012-0308-x.

[13] R.L. Baldwin Vi, M. Liu, E.E. Connor, T.G. Ramsay, G.E. Liu, C.-J. Li, Transcriptional reprogramming in rumen epithelium during the developmental transition of pre-ruminant to the ruminant in cattle, Animals (Basel) 11 (2021), https://doi.org/10.3390/ani11102870.

[14] N. Malmuthuge, G. Liang, L.L. Guan, Regulation of rumen development in neonatal ruminants through microbial metagenomes and host transcriptomes, Genome Biol. 20 (2019) 172, https://doi.org/10.1186/s13059-019-1786-0.

[15] S. Wu, Z. Cui, X. Chen, L. Zheng, H. Ren, D. Wang, J. Yao, Diet-ruminal microbiome-host crosstalk contributes to differential effects of calf starter and alfalfa hay on rumen epithelial development and pancreatic α-amylase activity in yak calves, J. Dairy Sci. 104 (2021) 4326–4340, https://doi.org/10.3168/jds.2020-18736.

[16] C.F. de Assis Lage, S.E. Räisänen, A. Melgar, K. Nedelkov, X. Chen, J. Oh, M. E. Fetter, N. Indugu, J.S. Bender, B. Vecchiarelli, M.L. Hennessy, D. Pitta, A. N. Hristov, Comparison of two sampling techniques for evaluating ruminal fermentation and microbiota in the planktonic phase of rumen digesta in dairy cows, Front. Microbiol. 11 (2020), 618032, https://doi.org/10.3389/fmicb.2020.618032.

[17] N. Malmuthuge, M. Li, Y. Chen, P. Fries, P.J. Griebel, B. Baurhoo, X. Zhao, L. L. Guan, Distinct commensal bacteria associated with ingesta and mucosal epithelium in the gastrointestinal tracts of calves and chickens, FEMS Microbiol. Ecol. 79 (2012) 337–347, https://doi.org/10.1111/j.1574-6941.2011.01220.x.

[18] N. Malmuthuge, P.J. Griebel, L.L. Guan, Taxonomic identification of commensal bacteria associated with the mucosa and digesta throughout the gastrointestinal tracts of preweaned calves, Appl. Environ. Microbiol. 80 (2014) 2021–2028, https://doi.org/10.1128/aem.03864-13.

[19] S. Mao, M. Zhang, J. Liu, W. Zhu, Characterising the bacterial microbiota across the gastrointestinal tracts of dairy cattle: membership and potential function, Sci. Rep. 5 (2015), https://doi.org/10.1038/srep16116.

[20] M. Zeineldin, J. Lowe, B. Aldridge, Contribution of the mucosal microbiota to bovine respiratory health, Trends Microbiol. 27 (2019) 753–770, https://doi.org/10.1016/j.tim.2019.04.005.

[21] R.S.G. Tan, M. Zhou, F. Li, L.L. Guan, Identifying active rumen epithelial associated bacteria and archaea in beef cattle divergent in feed efficiency using total RNA-seq, Curr. Res. Microb. Sci. 2 (2021), 100064, https://doi.org/10.1016/j.crmicr.2021.100064.

[22] W. Guo, J.K. van Niekerk, M. Zhou, M.A. Steele, L.L. Guan, Longitudinal assessment revealed the shifts in rumen and colon mucosal-attached microbiota of dairy calves during weaning transition, J. Dairy Sci. 104 (2021) 5948–5963, https://doi.org/10.3168/jds.2020-19252.

[23] M.L. Bainbridge, L.M. Cersosimo, A.-D.G. Wright, J. Kraft, Rumen bacterial communities shift across a lactation in Holstein, Jersey and Holstein × Jersey dairy cows and correlate to rumen function, bacterial fatty acid composition and production parameters, FEMS Microbiol. Ecol. 92 (2016) fiw059, https://doi.org/10.1093/femsec/fiw059.

[24] H. Shen, Z. Chen, Z. Shen, Z. Lu, Maintaining stability of the rumen ecosystem is associated with changes of microbial composition and epithelial TLR signaling, Microbiologyopen 6 (2017), https://doi.org/10.1002/mbo3.436.

[25] P. Langfelder, S. Horvath, WGCNA: an R package for weighted correlation network analysis, BMC Bioinform. 9 (2008) 559, https://doi.org/10.1186/1471-2105-9-559.

[26] E.D. Olfert, B.M. Cross, A.A. McWilliam, Guide to the Care and Use of Experimental Animals. https://neuron.mefst.hr/docs/graduate_school/tribe/Nastavni%20materijali/AnimalCourse/General/CCAC_Experimental_Animals_Vol1.pdf, 1993.

[27] J.K. van Niekerk, M. Middeldorp, M.A. Steele, Technical note: the development of a methodology for ruminal and colon tissue biopsying of young Holstein dairy calves, J. Dairy Sci. 101 (2018) 7212–7218, https://doi.org/10.3168/jds.2018-14374.

[28] A. Cánovas, G. Rincón, A. Islas-Trejo, R. Jimenez-Flores, A. Laubscher, J. F. Medrano, RNA sequencing to study gene expression and single nucleotide polymorphism variation associated with citrate content in cow milk, J. Dairy Sci. 96 (2013) 2637–2648, https://doi.org/10.3168/jds.2012-6213.

[29] A. Cánovas, A. Reverter, K.L. DeAtley, R.L. Ashley, M.L. Colgrave, M.R.S. Fortes, A. Islas-Trejo, S. Lehnert, L. Porto-Neto, G. Rincón, G.A. Silver, W.M. Snelling, J. F. Medrano, M.G. Thomas, Multi-tissue omics analyses reveal molecular regulatory networks for puberty in composite beef cattle, PLoS One 9 (2014), e102551, https://doi.org/10.1371/journal.pone.0102551.

[30] Babraham bioinformatics, FastQC A Quality Control Tool for High Throughput Sequence Data. https://www.bioinformatics.babraham.ac.uk/projects/fastqc/, 2010 (accessed January 3, 2023).

[31] E. Aronesty, Comparison of sequencing utility programs, Open Bioinform. J. 7 (2013) 1–8, https://doi.org/10.2174/1875036201307010001.

[32] A.V. Zimin, A.L. Delcher, L. Florea, D.R. Kelley, M.C. Schatz, D. Puiu, F. Hanrahan, G. Pertea, C.P. Van Tassell, T.S. Sonstegard, G. Marçais, M. Roberts, P. Subramanian, J.A. Yorke, S.L. Salzberg, A whole-genome assembly of the domestic cow, *Bos taurus*, Genome Biol. 10 (2009) R42, https://doi.org/10.1186/gb-2009-10-4-r42.

[33] D. Kim, G. Pertea, C. Trapnell, H. Pimentel, R. Kelley, S.L. Salzberg, TopHat2: accurate alignment of transcriptomes in the presence of insertions, deletions and gene fusions, Genome Biol. 14 (2013) R36, https://doi.org/10.1186/gb-2013-14-4-r36.

[34] B. Langmead, S.L. Salzberg, Fast gapped-read alignment with bowtie 2, Nat. Methods 9 (2012) 357–359, https://doi.org/10.1038/nmeth.1923.

[35] H. Li, B. Handsaker, A. Wysoker, T. Fennell, J. Ruan, N. Homer, G. Marth, G. Abecasis, R. Durbin, 1000 genome project data processing subgroup, the sequence alignment/map format and SAMtools, Bioinformatics 25 (2009) 2078–2079, https://doi.org/10.1093/bioinformatics/btp352.

[36] S. Anders, P.T. Pyl, W. Huber, HTSeq—a Python framework to work with high-throughput sequencing data, Bioinformatics 31 (2014) 166–169, https://doi.org/10.1093/bioinformatics/btu638.

[37] A. Cánovas, G. Rincón, C. Bevilacqua, A. Islas-Trejo, P. Brenaut, R.C. Hovey, M. Boutinaud, C. Morgenthaler, M.K. VanKlompenberg, P. Martin, J.F. Medrano, Comparison of five different RNA sources to examine the lactating bovine mammary gland transcriptome using RNA-sequencing, Sci. Rep. 4 (2014) 5297, https://doi.org/10.1038/srep05297.

[38] M.L. Smith, S. Durinck, W. Huber, Accessing Ensembl Annotation with Biomart. https://bioconductor.org/packages/release/bioc/vignettes/biomaRt/inst/doc/accessing_ensembl.html, 2022 (accessed September 12, 2022).

[39] Chen, McCarthy, Ritchie, Robinson, edgeR: Differential Analysis of Sequence Read Count Data User's Guide, Accessed. https://s3.jcloud.sjtu.edu.cn/899a892efef34b1b944a19981040f55b-oss01/bioconductor/3.13/bioc/vignettes/edgeR/inst/doc/edgeRUsersGuide.pdf, 2008.

[40] P.A.S. Fonseca, A. Suárez-Vega, A. Cánovas, Weighted gene correlation network meta-analysis reveals functional candidate genes associated with high- and sub-fertile reproductive performance in beef cattle, Genes 11 (2020), https://doi.org/10.3390/genes11050543.

[41] P.A. de Souza Fonseca, A. Suárez-Vega, A. Cánovas, Unrevealing functional candidate genes for bovine fertility through RNA sequencing meta-analysis and regulatory elements networks of co-expressed genes and lncRNAs, Funct. Integr. Genomics 22 (2022) 1361–1376, https://doi.org/10.1007/s10142-022-00893-1.

[42] H. Mi, A. Muruganujan, X. Huang, D. Ebert, C. Mills, X. Guo, P.D. Thomas, Protocol update for large-scale genome and gene function analysis with the PANTHER classification system (v.14.0), Nat. Protoc. 14 (2019) 703–721, https://doi.org/10.1038/s41596-019-0128-8.
[43] B.T. Sherman, M. Hao, J. Qiu, X. Jiao, M.W. Baseler, H.C. Lane, T. Imamichi, W. Chang, DAVID: a web server for functional enrichment analysis and functional annotation of gene lists (2021 update), Nucleic Acids Res. 50 (2022) W216–W221, https://doi.org/10.1093/nar/gkac194.
[44] V. Asselstine, F. Miglior, A. Suárez-Vega, P.A.S. Fonseca, B. Mallard, N. Karrow, A. Islas-Trejo, J.F. Medrano, A. Cánovas, Genetic mechanisms regulating the host response during mastitis, J. Dairy Sci. 102 (2019) 9043–9059, https://doi.org/10.3168/jds.2019-16504.
[45] A. Cánovas, R.N. Pena, D. Gallardo, O. Ramírez, M. Amills, R. Quintanilla, Segregation of regulatory polymorphisms with effects on the gluteus medius transcriptome in a purebred pig population, PLoS One 7 (2012), e35583, https://doi.org/10.1371/journal.pone.0035583.
[46] S. Zhao, Y. Guo, Y. Shyr, KEGGprofile: an annotation and visualization package for multi-types and multi-groups expression data in KEGG pathway, in: R Package Version, 2012.
[47] Harrell, Dupont, Hmisc: Harrell miscellaneous, in: R Package Version 4.1-1, … R-Project. Org/Package= Hmisc, 2004.
[48] Kolde Kolde, Package "Pheatmap," R Package. https://cran.microsoft.com/snapshot/2018-06-22/web/packages/pheatmap/pheatmap.pdf, 2018.
[49] M.A. Lane, R.L. Baldwin 6th, B.W. Jesse, Sheep rumen metabolic development in response to age and dietary treatments, J. Anim. Sci. 78 (2000) 1990–1996, https://doi.org/10.2527/2000.7871990x.
[50] D. Kirat, J. Masuoka, H. Hayashi, H. Iwano, H. Yokota, H. Taniyama, S. Kato, Monocarboxylate transporter 1 (MCT1) plays a direct role in short-chain fatty acids absorption in caprine rumen, J. Physiol. 576 (2006) 635–647, https://doi.org/10.1113/jphysiol.2006.115931.
[51] M.R. Waldron, F.N. Schrick, J.D. Quigley, J.L. Klotz, A.M. Saxton, R.N. Heitmann, Volatile fatty acid metabolism by epithelial cells isolated from different areas of the ewe rumen, J. Anim. Sci. 80 (2002) 270–278, https://doi.org/10.2527/2002.801270x.
[52] N. Schlau, L.L. Guan, M. Oba, The relationship between rumen acidosis resistance and expression of genes involved in regulation of intracellular pH and butyrate metabolism of ruminal epithelial cells in steers, J. Dairy Sci. 95 (2012) 5866–5875, https://doi.org/10.3168/jds.2011-5167.
[53] S.L. Alper, A.K. Sharma, The SLC26 gene family of anion transporters and channels, Mol. Asp. Med. 34 (2013) 494–515, https://doi.org/10.1016/j.mam.2012.07.009.
[54] D. Wang, S.M. King, T.A. Quill, L.K. Doolittle, D.L. Garbers, A new sperm-specific Na+/H+ exchanger required for sperm motility and fertility, Nat. Cell Biol. 5 (2003) 1117–1122, https://doi.org/10.1038/ncb1072.
[55] D. Kirat, K.I. Sallam, S. Kato, Expression and cellular localization of monocarboxylate transporters (MCT2, MCT7, and MCT8) along the cattle gastrointestinal tract, Cell Tissue Res. 352 (2013) 585–598, https://doi.org/10.1007/s00441-013-1570-5.
[56] E.E. Connor, R.W. Li, R.L. Baldwin, C. Li, Gene expression in the digestive tissues of ruminants and their relationships with feeding and digestive processes, Animal 4 (2010) 993–1007, https://doi.org/10.1017/S1751731109991285.
[57] L. Yan, B. Zhang, Z. Shen, Dietary modulation of the expression of genes involved in short-chain fatty acid absorption in the rumen epithelium is related to short-chain fatty acid concentration and pH in the rumen of goats, J. Dairy Sci. 97 (2014) 5668–5675, https://doi.org/10.3168/jds.2013-7807.
[58] C.C. Chang, H.Y. Huh, K.M. Cadigan, T.Y. Chang, Molecular cloning and functional expression of human acyl-coenzyme a:cholesterol acyltransferase cDNA in mutant Chinese hamster ovary cells, J. Biol. Chem. 268 (1993) 20747–20755. https://www.ncbi.nlm.nih.gov/pubmed/8407899.
[59] R.J. Kern, C.M. Zarek, A.K. Lindholm-Perry, L.A. Kuehn, W.M. Snelling, H. C. Freetly, H.C. Cunningham, A.M. Meyer, Ruminal expression of the NQO1, RGS5, and ACAT1 genes may be indicators of feed efficiency in beef steers, Anim. Genet. 48 (2017) 90–92, https://doi.org/10.1111/age.12490.
[60] M.A. Lane, R.L. Baldwin 4th, B.W. Jesse, Developmental changes in ketogenic enzyme gene expression during sheep rumen development, J. Anim. Sci. 80 (2002) 1538–1544, https://doi.org/10.2527/2002.8061538x.
[61] C. Zhao, K. Dahlman-Wright, Liver X receptor in cholesterol metabolism, J. Endocrinol. 204 (2010) 233–240, https://doi.org/10.1677/joe-09-0271.
[62] S. Murthy, E. Born, S.N. Mathur, F.J. Field, LXR/RXR activation enhances basolateral efflux of cholesterol in CaCo-2 cells, J. Lipid Res. 43 (2002) 1054–1064, https://doi.org/10.1194/jlr.m100358-jlr200.
[63] M.A. Steele, G. Vandervoort, O. AlZahal, S.E. Hook, J.C. Matthews, B.W. McBride, Rumen epithelial adaptation to high-grain diets involves the coordinated regulation of genes involved in cholesterol homeostasis, Physiol. Genomics 43 (2011) 308–316, https://doi.org/10.1152/physiolgenomics.00117.2010.
[64] J.R. Wright, Immunomodulatory functions of surfactant, Physiol. Rev. 77 (1997) 931–962, https://doi.org/10.1152/physrev.1997.77.4.931.
[65] B. Leighton, A.R. Nicholas, C.I. Pogson, The pathway of ketogenesis in rumen epithelium of the sheep, Biochem. J. 216 (1983) 769–772, https://doi.org/10.1042/bj2160769.
[66] R.L. Baldwin 6th, Use of isolated ruminal epithelial cells in the study of rumen metabolism, J. Nutr. 128 (1998) 293S–296S, https://doi.org/10.1093/jn/128.2.293S.
[67] I.A. Schulkens, K.C.M. Castricum, E.M. Weijers, P. Koolwijk, A.W. Griffioen, V. L. Thijssen, Expression, regulation and function of human metallothioneins in endothelial cells, J. Vasc. Res. 51 (2014) 231–238, https://doi.org/10.1159/000365550.
[68] D. Ross, D. Siegel, The diverse functionality of NQO1 and its roles in redox control, Redox Biol. 41 (2021), 101950, https://doi.org/10.1016/j.redox.2021.101950.
[69] X. Li, Z. Xun, Y. Yang, Inhibition of phosphoserine phosphatase enhances the anticancer efficacy of 5-fluorouracil in colorectal cancer, Biochem. Biophys. Res. Commun. 477 (2016) 633–639, https://doi.org/10.1016/j.bbrc.2016.06.112.
[70] M. Bensellam, M.K. Montgomery, J. Luzuriaga, J.Y. Chan, D.R. Laybutt, Inhibitor of differentiation proteins protect against oxidative stress by regulating the antioxidant–mitochondrial response in mouse beta cells, Diabetologia 58 (2015) 758–770, https://doi.org/10.1007/s00125-015-3503-1.
[71] J.D. Hayes, D.J. Pulford, The glut athione S-transferase supergene family: regulation of GST and the contribution of the lsoenzymes to cancer chemoprotection and drug resistance part I, Crit. Rev. Biochem. Mol. Biol. 30 (1995) 445–520, https://doi.org/10.3109/10409239509083491.
[72] L. Romero, K. Andrews, L. Ng, K. O'Rourke, A. Maslen, G. Kirby, Human GSTA1-1 reduces c-Jun N-terminal kinase signalling and apoptosis in Caco-2 cells, Biochem. J. 400 (2006) 135–141, https://doi.org/10.1042/BJ20060110.
[73] A. Raza, G. Dikdan, K.K. Desai, A. Shareef, H. Fernandes, V. Aris, A.N. de la Torre, D. Wilson, A. Fisher, P. Soteropoulos, B. Koneru, Global gene expression profiles of ischemic preconditioning in deceased donor liver transplantation, Liver Transpl. 16 (2010) 588–599, https://doi.org/10.1002/lt.22049.
[74] R. Chis, P. Sharma, N. Bousette, T. Miyake, A. Wilson, P.H. Backx, A.O. Gramolini, α-Crystallin B prevents apoptosis after H2O2 exposure in mouse neonatal cardiomyocytes, Am. J. Physiol. Heart Circ. Physiol. 303 (2012) H967–H978, https://doi.org/10.1152/ajpheart.00040.2012.
[75] J. Duan, L. Chen, H. Gao, T. Zhen, H. Li, J. Liang, F. Zhang, H. Shi, A. Han, GALNT6 suppresses progression of colorectal cancer, Am. J. Cancer Res. 8 (2018) 2419–2435. https://www.ncbi.nlm.nih.gov/pubmed/30662801.
[76] K. Wang, C. Li, X. Lin, H. Sun, R. Xu, Q. Li, Y. Wei, Y. Li, J. Qian, C. Liu, Q. Zhang, S. Yu, Z. Cui, X. Huang, B. Zhu, J. Zhou, C. Mao, Correction: targeting alkaline ceramidase 3 alleviates the severity of nonalcoholic steatohepatitis by reducing oxidative stress, Cell Death Dis. 11 (2020), https://doi.org/10.1038/s41419-020-2396-1.
[77] A. Bachem, C. Makhlouf, K.J. Binger, D.P. de Souza, D. Tull, K. Hochheiser, P. G. Whitney, D. Fernandez-Ruiz, S. Dähling, W. Kastenmüller, J. Jönsson, E. Gressier, A.M. Lew, C. Perdomo, A. Kupz, W. Figgett, F. Mackay, M. Oleshansky, B.E. Russ, I.A. Parish, A. Kallies, M.J. McConville, S.J. Turner, T. Gebhardt, S. Bedoui, Microbiota-derived short-chain fatty acids promote the memory potential of antigen-activated CD8+ T cells, Immunity 51 (2019) 285–297, e5, https://doi.org/10.1016/j.immuni.2019.06.002. e5.
[78] D. Nolfi-Donegan, A. Braganza, S. Shiva, Mitochondrial electron transport chain: oxidative phosphorylation, oxidant production, and methods of measurement, Redox Biol. 37 (2020), 101674, https://doi.org/10.1016/j.redox.2020.101674.
[79] K. Kannan, S.K. Jain, Oxidative stress and apoptosis, Pathophysiology 7 (2000) 153–163, https://doi.org/10.1016/s0928-4680(00)00053-5.
[80] B. Cai, S.H. Chang, E.B.E. Becker, A. Bonni, Z. Xia, p38 MAP kinase mediates apoptosis through phosphorylation of BimEL at Ser-65, J. Biol. Chem. 281 (2006) 25215–25222, https://doi.org/10.1074/jbc.M512627200.
[81] J. Kralova, M. Dvorak, M. Koc, V. Kral, p38 MAPK plays an essential role in apoptosis induced by photoactivation of a novel ethylene glycol porphyrin derivative, Oncogene 27 (2008) 3010–3020, https://doi.org/10.1038/sj.onc.1210960.
[82] J. Mentschel, R. Leiser, C. Mülling, C. Pfarrer, R. Claus, Butyric acid stimulates rumen mucosa development in the calf mainly by a reduction of apoptosis, Arch. Tierernahr. 55 (2001) 85–102, https://doi.org/10.1080/17450390109386185.
[83] D.M. Sun, S.Y. Mao, W.Y. Zhu, J.H. Liu, Effect of starter diet supplementation on rumen epithelial morphology and expression of genes involved in cell proliferation and metabolism in pre-weaned lambs, Animal 12 (2018) 2274–2283, https://doi.org/10.1017/S1751731118000290.
[84] X.-L. Su, Q. Tian, J. Zhang, X.-Z. Yuan, X.-S. Shi, R.-B. Guo, Y.-L. Qiu, Acetobacteroides hydrogenigenes gen. nov., sp. nov., an anaerobic hydrogen-producing bacterium in the family Rikenellaceae isolated from a reed swamp, Int. J. Syst. Evol. Microbiol. 64 (2014) 2986–2991, https://doi.org/10.1099/ijs.0.063917-0.
[85] X. Qiu, X. Qin, L. Chen, Z. Chen, R. Hao, S. Zhang, S. Yang, L. Wang, Y. Cui, Y. Li, Y. Ma, B. Cao, H. Su, Serum biochemical parameters, rumen fermentation, and rumen bacterial communities are partly driven by the breed and sex of cattle when fed high-grain diet, Microorganisms 10 (2022), https://doi.org/10.3390/microorganisms10020323.
[86] Y. Song, N. Malmuthuge, M.A. Steele, L.L. Guan, Shift of hindgut microbiota and microbial short chain fatty acids profiles in dairy calves from birth to pre-weaning, FEMS Microbiol. Ecol. 94 (2018), https://doi.org/10.1093/femsec/fix179.
[87] Z. Zhong, Y. Zhang, X. Li, L. Li, R. Zhang, S. Zhang, Differential responses of digesta- and mucosa-associated jejunal microbiota of Hu sheep to pelleted and non-pelleted high-grain diets, Animals 12 (2022) 1695, https://doi.org/10.3390/ani12131695.
[88] I. Rabbani, H. Rehman, H. Martens, K.A. Majeed, M.S. Yousaf, Z.U. Rehman, Carbonic anhydrase influences asymmetric sodium and acetate transport across omasum of sheep, Anim. Biosci. 34 (2021) 880–885, https://doi.org/10.5713/ajas.20.0163.
[89] E. Mann, S.U. Wetzels, M. Wagner, Q. Zebeli, S. Schmitz-Esser, Metatranscriptome sequencing reveals insights into the gene expression and functional potential of rumen wall bacteria, Front. Microbiol. 9 (2018) 43, https://doi.org/10.3389/fmicb.2018.00043.
[90] J. Jiao, J. Huang, C. Zhou, Z. Tan, Taxonomic identification of ruminal epithelial bacterial diversity during rumen development in goats, Appl. Environ. Microbiol. 81 (2015) 3502–3509, https://doi.org/10.1128/aem.00203-15.